

## Title page

ARHGAP24 represses  $\beta$ -catenin transactivation-induced invasiveness in hepatocellular carcinoma mainly by acting as a GTPase-independent scaffold

Wenjing Yang<sup>1\*</sup>, Beili Wang<sup>1,3,4\*</sup>, Qian Yu<sup>1,5\*</sup>, Te Liu<sup>6</sup>, Tong Li<sup>1</sup>, Tongtong Tian<sup>1</sup>, Anli Jin<sup>1</sup>, Lin Ding<sup>1</sup>, Wei Chen<sup>1</sup>, Hao Wang<sup>1</sup>, Jingrong Xian<sup>1</sup>, Baishen Pan<sup>1,3</sup>, Jian Zhou<sup>2,3</sup>, Jia Fan<sup>2,3</sup>, Xinrong Yang<sup>2,3#</sup>, Wei Guo<sup>1,3,4,5#</sup>

<sup>1</sup>Department of Laboratory Medicine, Zhongshan Hospital, Fudan University, Shanghai 200032, P. R. China.

<sup>2</sup>Department of Liver Surgery & Transplantation, Liver Cancer Institute, Zhongshan Hospital, Fudan University; Key Laboratory of Carcinogenesis and Cancer Invasion, Ministry of Education, Shanghai 200032, P. R. China.

<sup>3</sup>Cancer Center, Zhongshan Hospital, Fudan University, Shanghai 200032, P. R. China.

<sup>4</sup>Department of Laboratory Medicine, Xiamen Branch, Zhongshan Hospital, Fudan University, Xiamen 361015, P. R. China.

<sup>5</sup>Department of Laboratory Medicine, Wusong Branch, Zhongshan Hospital, Fudan University, Shanghai 200940, P. R. China.

<sup>6</sup>Shanghai Geriatric Institute of Chinese Medicine, Shanghai University of Traditional Chinese Medicine, Shanghai 200031, P. R. China.

\*These authors contributed equally.

## **Contact information**

Wei Guo (Corresponding author)

Department of Laboratory Medicine, Zhongshan Hospital, Fudan University,  
Shanghai 200032, China.

Tel & Fax: +86-21-64041990-2376

Email: [guo.wei@zs-hospital.sh.cn](mailto:guo.wei@zs-hospital.sh.cn)

Or to

Xin-Rong Yang (Corresponding author)

Department of Liver Surgery, Liver Cancer Institute, Zhongshan Hospital,  
Fudan University, 136 Yi Xue Yuan Road, Shanghai 200032, P. R. China.

Tel. & Fax: +86-21-64037181.

E-mail: [yang.xinrong@zs-hospital.sh.cn](mailto:yang.xinrong@zs-hospital.sh.cn)

## Supplementary Figures

**Supplementary figure 1. Low ARHGAP24 expression indicates the poorer prognosis of HCC patients.** **A.** Kaplan-Meier analysis of the overall survival (OS) in HCC patients stratified by ARHGAP24 expression according to K-M plotter dataset. **B.** Kaplan-Meier analysis of the relapse-free survival (RFS) in HCC patients stratified by ARHGAP24 expression according to K-M plotter dataset. **C.** Kaplan-Meier analysis of the progression-free survival (PFS) in HCC patients stratified by ARHGAP24 expression according to K-M plotter dataset. **D.** Kaplan-Meier analysis of the disease-specific survival (DSS) in HCC patients stratified by ARHGAP24 expression according to K-M plotter dataset.

**Supplementary figure 2. ARHGAP24 expression could predict the prognosis of HCC patients with high risk of recurrence.** **A.** Kaplan-Meier analysis of progression-free survival (PFS) of HCC patients with tumor size < 5 cm, with single tumor number, and with early tumor differentiation. **B.** Kaplan-Meier analysis of progression-free survival (PFS) of HCC patients with early tumor stage (Chinese liver tumor stage), without satellite lesions and without microvascular invasion. **C.** Univariate cox proportional regression analysis of factors associated with HCC tumor recurrence.

**Supplementary figure 3. Kaplan-Meier analysis for OS in other tumors. A.**

Kaplan-Meier analysis of the OS of kidney renal clear cell carcinoma in ARHGAP24 high expression group and ARHGAP24 low expression group. **B.** Kaplan-Meier analysis of the OS of lung adenocarcinoma in ARHGAP24 high expression group and ARHGAP24 low expression group. **C.** Kaplan-Meier analysis of the OS of pancreatic ductal adenocarcinoma in ARHGAP24 high expression group and ARHGAP24 low expression group. **D.** Kaplan-Meier analysis of the OS of kidney renal papillary cell carcinoma in ARHGAP24 high expression group and ARHGAP24 low expression group. **E.** Kaplan-Meier analysis of the OS of lung squamous cell carcinoma in ARHGAP24 high expression group and ARHGAP24 low expression group.

**Supplementary figure 4. ARHGAP24 overexpression inhibits huh7 cell proliferation.** **A.** Cell proliferation-related molecules were detected by WB assays in ARHGAP24 overexpressed-Huh7 cells. **B.** Effects of ARHGAP24 overexpression on huh7 cell proliferation using colony formation assays. **C.** Effects of ARHGAP24 overexpression on huh7 cell proliferation using CCK8 assays. **D.** Effects of ARHGAP24 knockdown on Li-7 cell cycle using flow cytometry. **E.** Effects of ARHGAP24 overexpression on Huh7 cell cycle using flow cytometry. **F.** Effects of ARHGAP24 overexpression on HCCLM3 cell cycle using flow cytometry. **G.** Effects of ARHGAP24 overexpression on Huh7 cell apoptosis using flow cytometry.

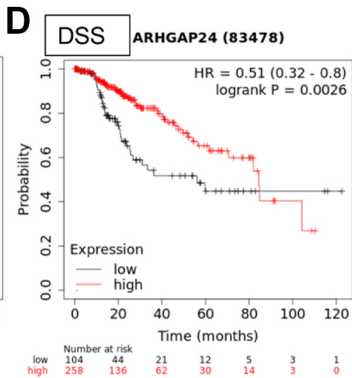
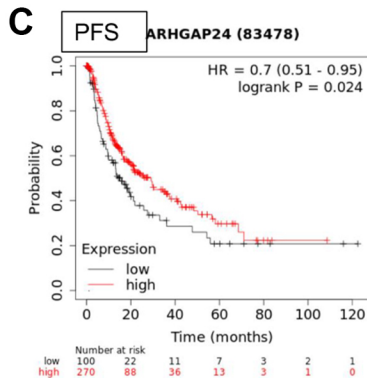
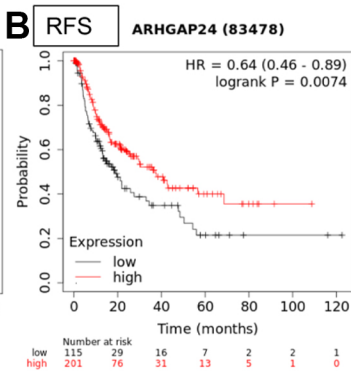
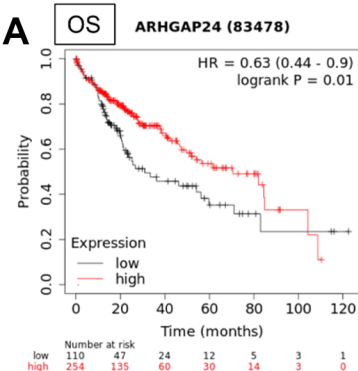
**Supplementary figure 5. ARHGAP24 inhibits cell invasiveness via inactivating wnt/ $\beta$ -catenin signaling pathway.** **A.** Effects of ARHGAP24 overexpression on Huh7 cell migration and invasion using Transwell assays. **B.** Effects of ARHGAP24 overexpression on Huh7 cell migration using scratch wound healing assays. **C.** qRT-PCR analysis of EMT-related markers in ARHGAP24 overexpressed Huh7 cells. **D.** Protein expression of EMT-related markers in ARHGAP24 overexpressed Huh7 cells. **E.** Protein expression of downstream target genes of  $\beta$ -catenin in ARHGAP24 overexpression and knockdown cells. **F.** Effects of ICG-001 on HCCLM3 cell proliferation using CCK8 assays. **G.** Effects of ICG-001 on sh-ARH Li-7 cell proliferation using CCK8 assays.

**Supplementary figure 6. ARHGAP24 inhibits cell invasiveness independent of Rho GTPase activity.** **A.** Q158R plasmids were successfully constructed and confirmed by sanger sequence analysis. **B.** Protein expressions of EMT-related markers in HCCLM3 cells transfected with the indicated plasmids. **C.** Protein expressions of EMT-related markers in Huh7 cells transfected with the indicated plasmids.

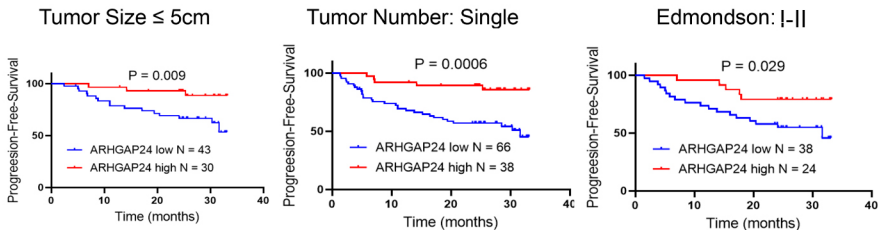
**Supplementary figure 7. ARHGAP24 inhibits HCC progression by degradation of PKM2.** **A.** PKM2 was successfully silenced in ARHGAP24 knockdown cells. **B.** Protein expressions of EMT-related markers were detected

by WB assays. **C.** Silenced PKM2 have no effects on increased Rho GTPase activity caused by knockdown ARHGAP24 in Li-7 cells. **D.** Effects of PKM2 silencing on HCCLM3 cell proliferation using CCK8 assays. **E.** Effects of PKM2 silencing on sh-ARH Li-7 cell proliferation using CCK8 assays.

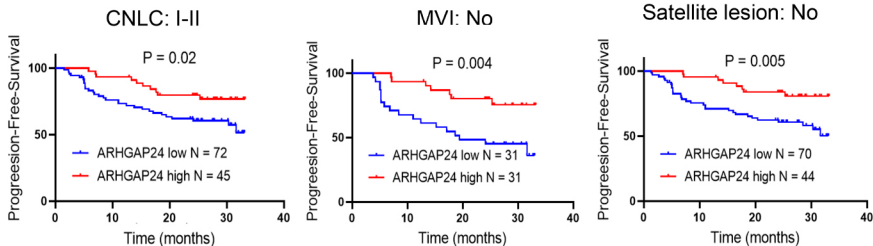
**Supplementary figure 8. ARHGAP24 recruits WWP1 to degrade PKM2. A.** IP and WB analyses of PKM2, WWP1 and ARHGAP24 protein expression in HCCLM3 and MHCC97H cells transfected with the numbers of ARHGAP24-HA plasmids. **B.** Representative pictures of the binding domain of the ARHGAP24 and PKM2 structure. **C.** IP and WB analyses and Ubiquitination assays of PKM2 in the presence or absence of ARHGAP24 C-terminal domain.



A

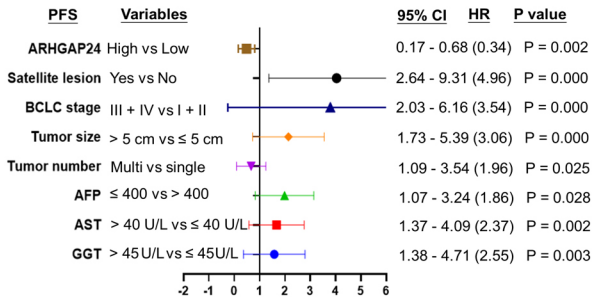


B



C

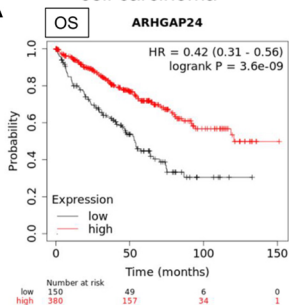
Univariate cox proportional regression analysis of factors associated with tumor recurrence



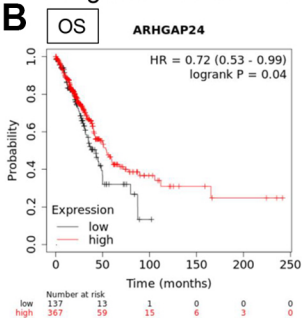


**A**

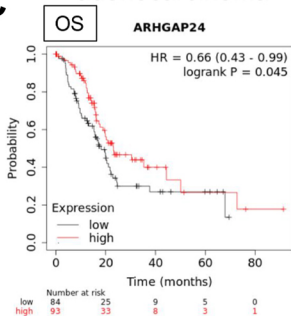
## Kidney renal clear cell carcinoma

**B**

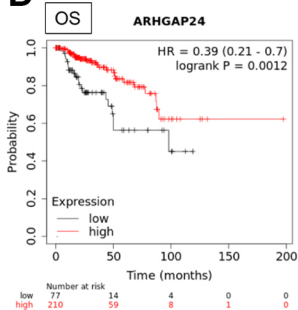
## Lung adenocarcinoma

**C**

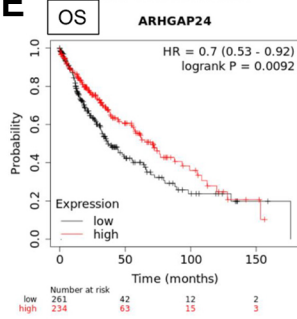
## Pancreatic ductal adenocarcinoma

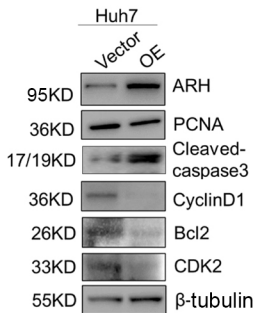
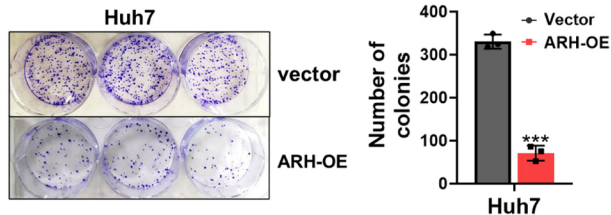
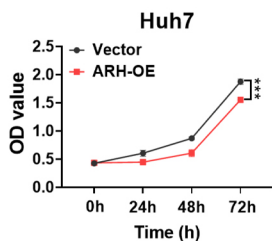
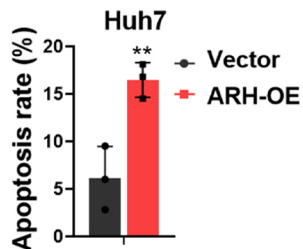
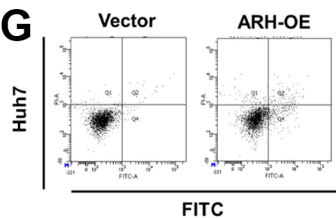
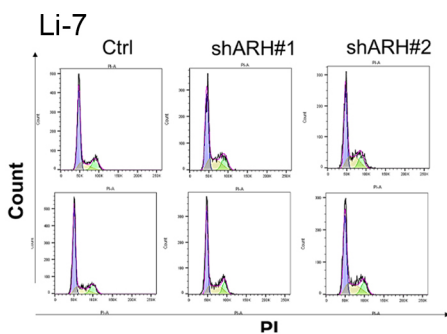
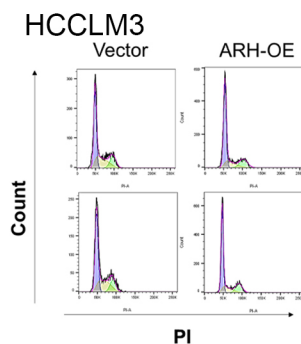
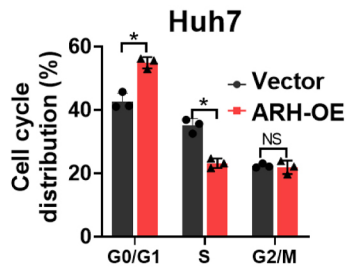
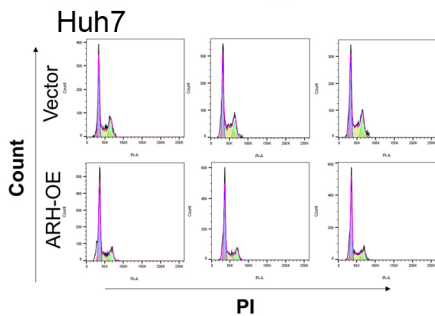
**D**

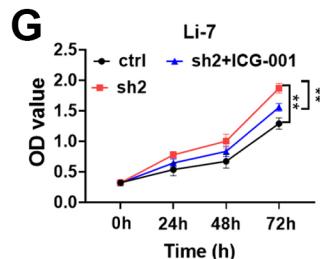
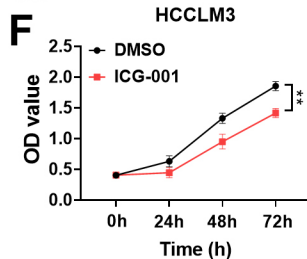
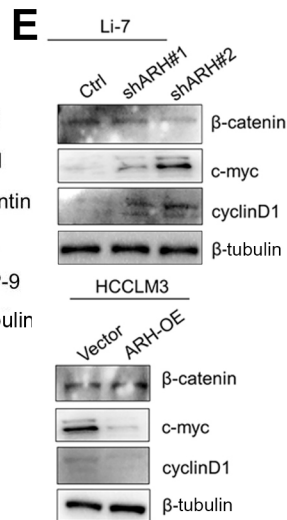
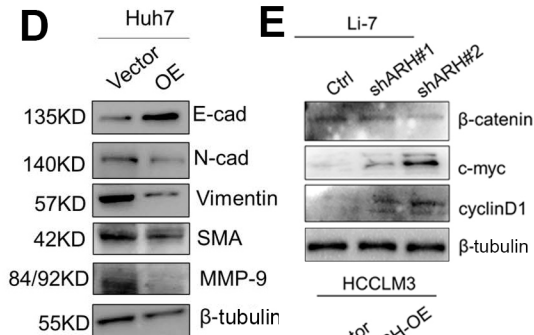
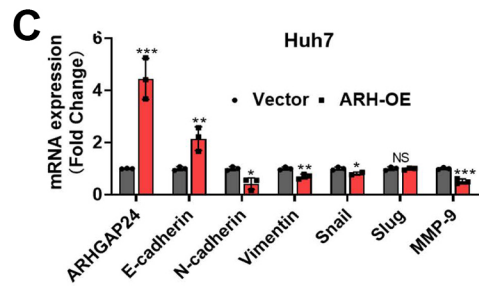
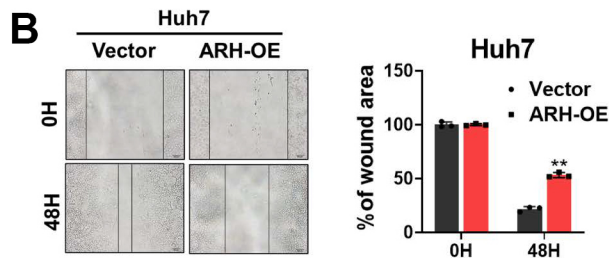
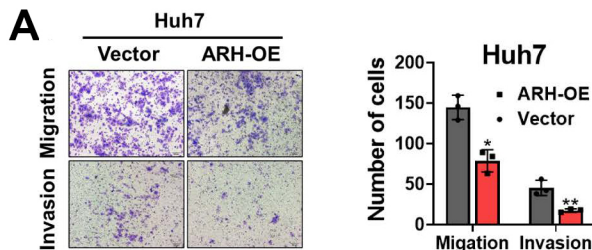
## Kidney renal papillary cell carcinoma

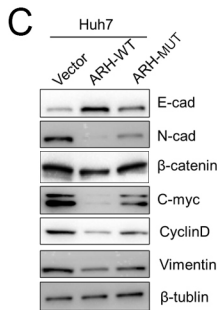
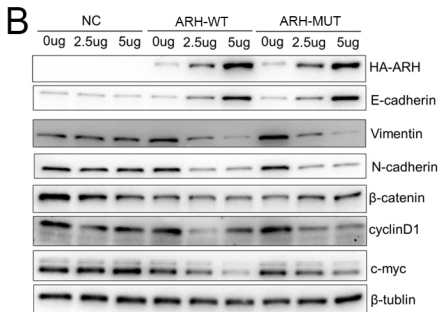
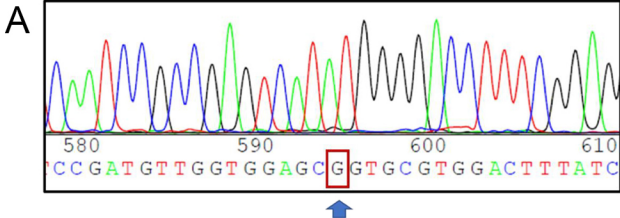
**E**

## Lung squamous cell carcinoma



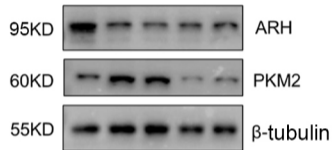
**A****B****C****G****D****F****E**



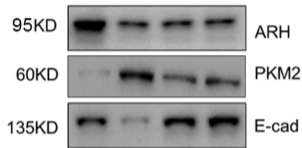


**A**

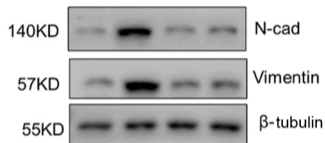
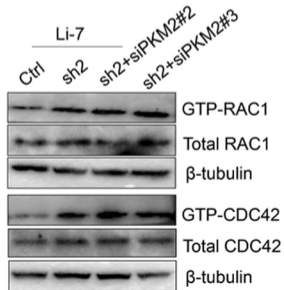
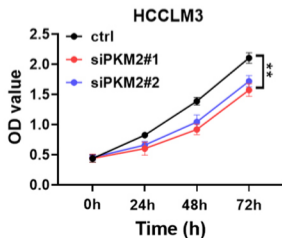
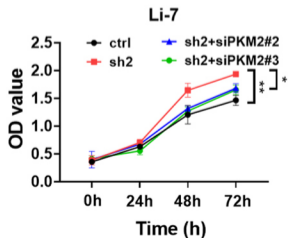
Ctrl	+	-	-	-	-
shARH#2	-	+	+	+	+
siPKM2#1	-	-	+	-	-
siPKM2#2	-	-	-	+	-
siPKM2#3	-	-	-	-	+

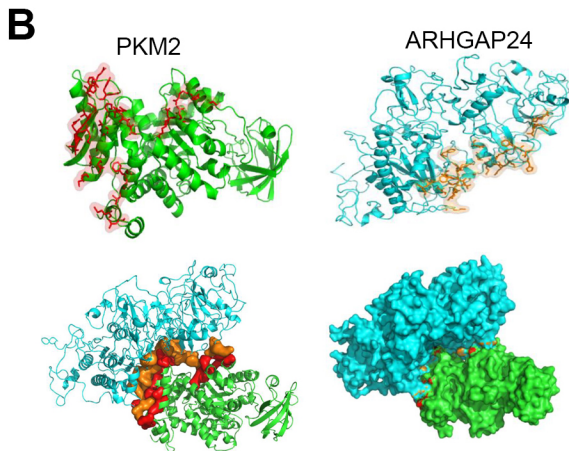
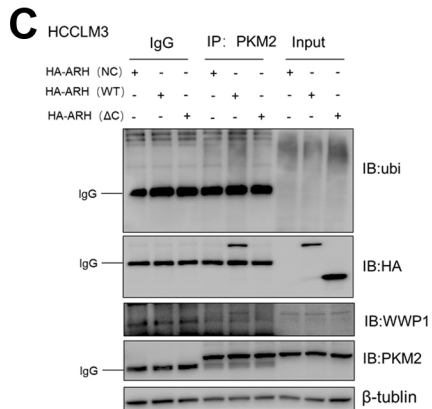
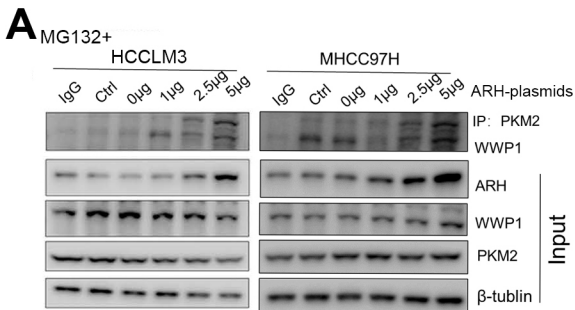
**B**

Ctrl	+	-	-	-
shARH#2	-	+	+	+
siPKM2#2	-	-	+	-
siPKM2#3	-	-	-	+



+	-	-	-
-	+	+	+
-	-	+	-
-	-	-	+

**C****D****E**



## **Supplementary Tables**

**Supplementary Table 1.** List of potential interactors of ARHGAP24 identified by IP-MS.

**Supplementary Table 2.** The correlations between ARHGAP24 expression and clinicopathological characteristics in HCC.

**Supplementary Table 3.** Univariate cox proportional regression analysis of factors associated with recurrence and overall survival.















774	tr A0A087WVM4 A0A087WVM4_HUMAN	29.27	99312	Monofunctional C1-tetrahydrofolate synthase mitochondrial OS=Homo sapiens OX=9606 GN=MTHFD1L PE=1 SV=1
775	sp Q6UB35 C1TM_HUMAN	29.27	105790	Monofunctional C1-tetrahydrofolate synthase mitochondrial OS=Homo sapiens OX=9606 GN=MTHFD1L PE=1 SV=1
776	tr B7ZM99 B7ZM99_HUMAN	29.27	105889	MTHFD1L protein OS=Homo sapiens OX=9606 GN=MTHFD1L PE=1 SV=1
777	tr A0A087WTT1 A0A087WTT1_HUMAN	29.04	58536	Polyadenylate-binding protein OS=Homo sapiens OX=9606 GN=PABPC1 PE=1 SV=1
778	tr E7EQV3 E7EQV3_HUMAN	29.04	65748	Polyadenylate-binding protein OS=Homo sapiens OX=9606 GN=PABPC1 PE=1 SV=1
779	sp P11940 PABP1_HUMAN	29.04	70671	Polyadenylate-binding protein 1 OS=Homo sapiens OX=9606 GN=PABPC1 PE=1 SV=2
780	tr H0YAR2 H0YAR2_HUMAN	29.04	32258	Polyadenylate-binding protein 1 (Fragment) OS=Homo sapiens OX=9606 GN=PABPC1 PE=1 SV=1
781	tr E7ERJ7 E7ERJ7_HUMAN	29.04	67139	Polyadenylate-binding protein OS=Homo sapiens OX=9606 GN=PABPC1 PE=1 SV=1
782	sp Q9H361 PABP3_HUMAN	29.04	70031	Polyadenylate-binding protein 3 OS=Homo sapiens OX=9606 GN=PABPC3 PE=1 SV=2
783	sp Q5VTR2 BRE1A_HUMAN	28.93	113662	E3 ubiquitin-protein ligase BRE1A OS=Homo sapiens OX=9606 GN=RNFB20 PE=1 SV=2
784	sp Q9Y4C4 MFHA1_HUMAN	28.81	116950	Malignant fibrous histiocytoma-amplified sequence 1 OS=Homo sapiens OX=9606 GN=MFHA1 PE=1 SV=2
785	tr D6RA20 D6RA20_HUMAN	28.81	97241	Protocadherin alpha-4 OS=Homo sapiens OX=9606 GN=PCDHA4 PE=1 SV=2
786	sp Q9UN74 PCDA4_HUMAN	28.81	102293	Protocadherin alpha-4 OS=Homo sapiens OX=9606 GN=PCDHA4 PE=1 SV=1
787	tr A0A087WSW8 A0A087WSW8_HUMAN	28.81	83615	Protocadherin alpha-4 OS=Homo sapiens OX=9606 GN=PCDHA4 PE=1 SV=1
788	sp P05154 PSP_HUMAN	28.75	45675	Plasma serine protease inhibitor OS=Homo sapiens OX=9606 GN=SERPINA5 PE=1 SV=3

**Supplementary Table 2.** The correlations between ARHGAP24 expression and clinicopathological characteristics in HCC.

		ARHGAP24 expression			P
		low (85)	High (46)		
Gender	Male	27	18 (66.7)	9 (33.3)	0.828
	Female	104	67 (64.4)	37 (35.6)	
Age	≤50	39	28 (71.8)	11 (28.2)	0.281
	>50	92	57 (62.0)	35 (38.0)	
Liver cirrhosis	No	64	45 (70.3)	19 (29.7)	0.203
	Yes	67	40 (59.7)	27 (40.3)	
HBsAg	No	27	17 (63.0)	10 (37.0)	0.814
	Yes	104	68 (65.4)	36 (34.6)	
ALT,U/L	≤40	101	62 (61.4)	39 (38.6)	0.124
	>40	30	23 (76.7)	7 (23.3)	
AST,U/L	≤40	88	55 (62.5)	33 (37.5)	0.413
	>40	43	30 (69.8)	13 (30.2)	
AFP, ng/ml	≤400	91	57 (62.6)	34 (37.4)	0.416
	>400	40	28 (70.0)	12 (30.0)	
Tumor number	Single	104	66 (63.5)	38 (36.5)	0.503
	Multiple	27	19 (70.4)	8 (29.6)	
Tumor size, cm	≤5	73	43 (58.9)	30 (41.1)	0.108
	>5	58	42 (72.4)	16 (27.6)	
Satellite lesion	No	114	70 (61.4)	44 (38.6)	<b>0.031</b>
	Yes	17	15 (88.2)	2 (11.8)	
MVI	No	62	31 (50.0)	31 (50.0)	<b>0.001</b>
	Yes	69	54 (78.3)	15 (21.7)	
Edmondson stage	I-II	62	38 (60.9)	24 (39.1)	0.414
	III-IV	69	47 (68.1)	22 (31.9)	
BCLC stage	0+A	100	61 (61.0)	39 (39.0)	0.094
	B+C	31	24 (77.4)	7 (22.6)	
CNLC stage	I-II	117	72 (61.5)	45 (38.5)	<b>0.020</b>
	III-IV	14	13 (92.9)	1 (7.1)	
Tumor recurrence	No	79	43 (54.4)	36 (45.6)	<b>0.002</b>
	Yes	52	42 (80.8)	10 (19.2)	

Abbreviations: ALT, alanine aminotransferase; AST, aspartate transaminase; AFP, α-fetoprotein; MVI, Microvascular invasion; BCLC, Barcelona Clinic Liver Cancer; CNLC, China liver cancer staging.

**Supplementary Table 3.** Univariate cox proportional regression analysis of factors associated with recurrence and overall survival

Variables	Tumor Recurrence	
	HR (95% CI)	P
Sex	0.69	
(Male versus female)	(0.37-1.30)	0.255
Age	1.37	
(>50 versus ≤50)	(0.73-2.56)	0.331
HBsAg	1.16	
(Yes versus No)	(0.57-2.38)	0.683
Liver cirrhosis	1.01	
(Yes versus no)	(0.58-1.73)	0.986
γ-GT, U/L	2.55	
(>45 versus ≤45)	1.38-4.71	<b>0.003</b>
ALT	1.48	
(>40U/L versus ≤40U/L)	(0.81-2.69)	0.205
AST	2.37	
(>40U/L versus ≤40U/L)	(1.37-4.09)	<b>0.002</b>
AFP	1.86	
(>400ng/ml versus ≤400ng/ml)	(1.07-3.24)	<b>0.028</b>
No. of tumors	1.96	
(Multi versus single)	(1.09-3.54)	<b>0.025</b>
Tumor size	3.06	
(>5cm versus ≤5cm)	(1.73-5.39)	<b>0.000</b>
Micro vascular invasion	1.05	
(Yes versus no)	(0.61-1.82)	0.852
Satellite lesion	4.96	
(Yes versus no)	(2.64-9.31)	<b>0.000</b>
Edmondson stage	1.29	
(III-IV versus I-II)	(0.75-2.24)	0.358
BCLC stage	3.54	
(B+C versus 0+A)	(2.03-6.16)	<b>0.000</b>
ARHGAP24	0.34	
(High versus low)	(0.17-0.68)	<b>0.002</b>

Abbreviations: ALT, alanine aminotransferase; AST, aspartate transaminase; AFP, α-fetoprotein; BCLC, Barcelona Clinic Liver Cancer; HR, hazard ratio.



## **Methods and Materials**

### **Cell culture**

Huh7, Li-7, and Hep3B cells were purchased from the Chinese Academy of Sciences Shanghai Branch Cell Bank (Shanghai, China). L02, MHCC97L, MHCC97H, and HCCLM3 cells were gifted by Professor Yang at the Liver Cancer Institute of Zhongshan Hospital, Fudan University. The cell lines were cultured in DMEM medium (Gibco, Grand Island, NY, USA) supplemented with 10% fetal bovine serum (Gibco) and penicillin/streptomycin, and maintained in an incubator at 37°C containing 5% CO<sub>2</sub>.

### **Generation of lentivirus and plasmid construction**

Wild-type ARHGAP24 for overexpression of ARHGAP24 (ARH-OE cells) and negative control vector (Vector) were transfected into HCCLM3 and Huh7 cells, based on the GV492 vector (Ubi-MCS-3Flag-CBh-IRES-puromycin) purchased from Shanghai Genechem Corporation (Shanghai, China). Knockdown lentiviral vector (shARH#1 and shARH#2) and negative control vector (NC) were transfected into Li-7 cells, based on the GV493 vector (Hu6-MCS-CBh-gcGFP-IRES-puromycin) purchased from Shanghai Genechem Corporation. SiPKM2 and siWWP1 were constructed by Shanghai GenePharma Corporation (Shanghai, China).

Full-length ARHGAP24, PKM2, and WWP1 plasmids were obtained by cloning cDNA into a phage vector with a corresponding HA, FLAG, or His tag. The GAP-deficient mutant of ARHGAP24 (HA-Q158R) and a series of ARHGAP24 mutations that lack different domains, including HA-ARH-PHD, HA-ARH-GAPD, HA-ARH-CD, and HA-ARH- $\Delta$ CD, and deletion mutants of PKM2, including Flag-PKM2- $\Delta$ CD, Flag-PKM2-ABD, and Flag-PKM2-CD, and deletion mutants of ARHGAP24 were constructed by Shanghai Genechem Corporation. ARHGAP24 mutants, including M1, M2, M3, and M4, were also designed by

Shanghai Genechem Corporation.

### **Western blot and Immunofluorescence**

Western blotting and immunofluorescence assays were performed as described previously [1]. Briefly, for western blot assays, proteins were extracted from the indicated cells and fractionated by SDS-PAGE. Then, proteins were transferred to nitrocellulose membranes. After blocking with 5% milk at room temperature for 1 h, the membranes were incubated with the specific primary antibodies overnight. For immunofluorescence assay, the cells were fixed, permeabilized, and blocked. Then, the indicated primary antibodies were incubated with cells. The next day, the membranes and cells were washed three times with PBS and incubated with a horseradish peroxidase-conjugated secondary antibody and fluorescently labeled secondary antibody, respectively. To observe the cytoskeleton, phalloidin was used for immunofluorescence staining.

### **Immunohistochemistry**

Immunohistochemical staining was performed as described previously [1]. Briefly, HCC tissues underwent the following steps: dewaxing treatment, antigen retrieval, and endogenous peroxidase blockade. The primary antibodies and dilutions used to detect the intensities of the indicated markers are listed below. Immunostaining intensities of the indicated markers were evaluated as follows: negative, weak, moderate and strong. When the intensity was negative or weak, the expression status was defined as “low expression”, while the intensity was moderate or strong, the expression status was defined as “high expression”. At least two pathology-related professionals interpreted the slices in a double-blind manner. If the results of the two personnel were disputed, other related pathology professionals examined the slice again. After discussion by all personnel, the final immunostaining group was determined.

## **Immunoprecipitation**

The indicated plasmids were co-transfected into Li-7, HCCLM3, and HEK293T cells. After 48 h, cells were lysed with IP lysis buffer (20mM Tris-HCL, pH7.4, 150mM NaCL, 1mM EDTA, and 1% NP-40) containing protease inhibitor cocktail (Roche, USA). Immunoprecipitation assays were performed following the manufacturer's instructions (Pierce, Thermo, USA). The supernatant protein was immunoprecipitated with the indicated tagged antibodies and protein G agarose beads overnight at 4°C. Antibodies used in these experiments are listed below. The complex was washed with NaCl buffer and boiled with 1×SDS loading buffer.

## **Antibodies and reagents**

Antibodies used in this study were ARHGAP24 (PA5-104104; Invitrogen),  $\beta$ -tubulin (Beyotime, Shanghai), PCNA (13110; Cell Signaling Technology), cleaved-caspase3 (9664; Cell Signaling Technology), cyclin D1 (55506; Cell Signaling Technology), BCL2 (15071; Cell Signaling Technology), CDK2 (18048; Cell Signaling Technology), E-cadherin (3195; Cell Signaling Technology), N-cadherin (13116; Cell Signaling Technology), vimentin (5741; Cell Signaling Technology),  $\alpha$ -SMA (19245; Cell Signaling Technology), MMP-9 (13667; Cell Signaling Technology), Ki67 (9449; Cell Signaling Technology),  $\beta$ -catenin (8480; Cell Signaling Technology), c-MYC (18583; Cell Signaling Technology), PKM2 (4053; Cell Signaling Technology), WWP1 (ab104440; Abcam), anti-FLAG (14793; Cell Signaling Technology), anti-HA (3724; Cell Signaling Technology), and anti-His (12698; Cell Signaling Technology).

## **Cell proliferation, migration, and invasion assays**

CCK8 and colony formation assays were used to investigate cell proliferation, which were performed as described previously [1]. Cell migration and invasion were detected using transwell chambers (BD, PharMingen, San Jose, CA), as

previously described [51]. Briefly,  $5 \times 10^4$  cells were plated in the top chamber with Matrigel used or not, and the lower chamber was supplemented with 500  $\mu$ L complete medium and incubated for 24 h. The next day, after fixing with methanol and staining with crystal violet, the cells on the membrane were counted on three inserts. Cell migration was also investigated by cell scratching assay, as previously described [1].

### **Cell cycle and cell apoptosis assays**

Flow cytometry (Aria II flow cytometer, BD, USA) was performed to analyze cell cycle and cell apoptosis, as described previously. For cell cycle analysis, cells were harvested and fixed with 70% ethanol overnight at 4°C. The cells were then washed three times, and 50  $\mu$ g/mL PI, 100  $\mu$ g/mL RNase A, and 0.2% Triton X-100 were added to each sample. For cell apoptosis analysis, control cells and experimental cells were seeded into 24-well plates and cultured for 48 h. Then, the cells were collected, resuspended, and treated with the Annexin V-FITC Apoptosis Detection Kit (BD, PharMingen, San Jose, CA) following the manufacturer's instructions. Briefly, 5  $\mu$ L FITC-labeled Annexin V and 5  $\mu$ L PI solution were added to each sample, and the cells were incubated for 15 min at room temperature.

### **In vivo assays**

Six-week-old BALB/C nude mice were purchased from the Shanghai Institute of Material Medicine of the Chinese Academy of Science (Shanghai, China). The committee on the use of live animals in teaching and research at Zhongshan Hospital, Fudan University, approved all animal experiments. Li-7-Ctrl, Li-7-shARH, HCCLM3-vector, and HCCLM3-ARH-OE cells ( $5 \times 10^6$ ) were suspended in 200  $\mu$ L serum-free DMEM and Matrigel (BD Biosciences; 1:1), and then injected subcutaneously into the flanks of nude mice. After 4 weeks, when the tumor volume had grown to 1 cm<sup>3</sup>, the mice were killed and the tumor tissue was stripped. Then, the center area of the tumor tissue was selected and

the necrotic tissue was removed. The tumor tissue was then cut to a size of 1–2 mm<sup>3</sup> for subsequent orthotopic transplantation tumor model construction. A total of 24 nude mice were selected and randomly assigned to four groups. After completion of the transplantation for 6 weeks, the mice were killed. The volume and weight of the tumor were measured. At the same time, the liver cancer tissues were embedded in paraffin for subsequent IHC analysis.

For tumor metastasis analysis, 6- to 8-week-old nude mice were selected and randomly assigned to four groups. Mice were injected with  $2 \times 10^6$  of the indicated cells via the tail vein. After 8 weeks, the lung tissues were separated and stained with HE. The numbers of tumor metastasis were recorded.

### **Ubiquitination analysis**

The indicated plasmids were co-transfected into Li-7, HCCLM3, and HEK293T cells. After incubation for 24 h, the cells were treated with 10  $\mu$ M MG132 for 6 h. Then, the cells were lysed with IP lysis buffer and boiled at 100°C for 10 min. The supernatants were collected and RIPA lysis was then added to PMSF and protease inhibitor cocktail for IP with anti-PKM2, anti-FLAG, anti-HA, or anti-His.

### **Bioinformatics**

For identification of DEGs and pathway enrichment, the FPKM and count expression profiles were obtained from the TCGA database (<https://portal.gdc.cancer.gov/>), UCSC Xena website (<http://xena.ucsc.edu/>), GEO database (<https://www.ncbi.nlm.nih.gov/geo/>) and the Clinical Proteomic Tumor Analysis Consortium (<https://proteomic.datacommons.cancer.gov/pdc/>). “limma” R package and GEO2R online tools were employed to perform differential expression analysis between tumor tissue and tumor adjacent tissues in the GSE164760, GSE76427, GSE101728, GSE101685, TCGA and CPTAC cohorts. TCGA-LIHC samples were divided into ARHGAP24 high and low expression groups based on the upper and lower quartiles of ARHGAP24

expression. Genes with an expression- p value < 0.05 and  $|\log_2$  fold change (FC)| >1 were regarded as significant DEGs using “limma” R package. To explore whether genes in ARHGAP24 high and low expression groups were enriched in meaningful biological processes, gene set enrichment analysis was performed in the two groups ([www.gsea-msigdb.org/gsea/index.jsp](http://www.gsea-msigdb.org/gsea/index.jsp)). The annotated gene set c2.cp.reactome.v7.5.1.symbols.gmt [Curated] was selected as the reference gene set. Visual analysis of data was generated by “ggplot2”, “pheatmap” and “enrichplot” R package. Follow-up data of patients with various cancers were acquired from the K-M plot database (<http://kmplot.com/analysis>). The CPTAC cohort follow-up information was acquired from the website <https://proteomics.cancer.gov/programs/cptac>.

For the analysis of the interaction between PKM2 and ARHGAP24, the three-dimensional protein structures of PKM (Uniport ID: P14618-1) and ARHGAP24 (Uniport ID: Q8N264-1) were established by the comprehensive use of multiple protein three-dimensional structure modeling software, including I-TASSER, FR-t5-M, and FALCON. The binding amino acid positions in the constructed PKM2 and ARHGAP24 three-dimensional protein structures were predicted by tools such as SPR and ISPRED4, respectively. According to the protein interaction sites, the optimal docking model was identified using HDOCK. MEFTop and QIPI were also used to evaluate the docking conformation. ContPro was used to calculate the spatial distance of each atom in the docking model, and 4Å was selected as the threshold of the distance between atoms to select the amino acids that may have interactions in the docking model.

### **TOP/FOP FLASH assays**

TOP/FOP flash analysis was performed in accordance with the manufacturer’s protocol (Sigma–Aldrich, USA). TOP flash (TCF reporter plasmid) and FOP flash (mutant TCF binding sites) were used. The indicated HCC cell lines were co-transfected with 100 ng reporter plasmid, 50 ng expression plasmid, and 8

ng *Renilla* luciferase plasmid with Lipo2000 in a 96-well plate. After 24 h, the luciferase reporters TOP/FOP FLASH were combined with the various expression plasmids. Finally, the indicated cells were analyzed using a luciferase reporter assay kit (Promega) and a microplate reader.

## **Reference**

[1] Yang W, Zhang C, Li Y, et al. Phosphorylase Kinase  $\beta$  Represents a Novel Prognostic Biomarker and Inhibits Malignant Phenotypes of Liver Cancer Cell. *Int J Biol Sci.* 2019;15(12):2596-2606.

**The targeting sequences of small hairpin RNAs were used in study.**

Gene	Target sequences
shRNA#1 against ARHGAP24	5'- ccGAGAGAGGAAACACAATAT -3'
shRNA#2 against ARHGAP24	5'- ccAGCAGTTGATGTCAGTGAT-3'
Scrambled shRNA	5'- TTCTCCGAACGTGTCACGT-3'
SiPKM2#1	Sense: 5'- GGAUGUUGAUAUGGUGUUUTT-3' Anti-sense: 5'- AAACACCAUAUCAACAUCCTT-3'
SiPKM2#2	Sense: 5'- CCAUCUACCACUUGCAAUUTT-3' Anti-sense: 5'- AAUUGCAAGUGGUAGAUGGTT-3'
SiWWP1#1	5'-GAAGTCATCTGTAACAAA-3'
SiWWP1#2	5'-GCAGAGAAATACTGTTTAT-3'

**The primer sequences were used in study.**

Gene		Sequences
ARHGAP24	Forward	5'- GAACCGTCTGGCTCCGATG -3'
	Reverse	5'- TGGCAGTCGAAAGAGACCCT -3'
CTNNB1	Forward	5'- AAAGCGGCTGTTAGTCACTGG-3'
	Reverse	5'- CGAGTCATTGCATACTGTCCAT-3'
PKM2	Forward	5'- ATGTCGAAGCCCCATAGTGAA-3'
	Reverse	5'- TGGGTGGTGAATCAATGTCCA-3'
E-cadherin	Forward	5'- CGAGAGCTACACGTTACCGG -3'
	Reverse	5'- GGGTGTGAGGGGAAAAATAGG-3'
N-cadherin	Forward	5'- TCAGGCGTCTGTAGAGGCTT-3'
	Reverse	5'- ATGCACATCCTTCGATAAGACTG-3'
vimentin	Forward	5'- GACGCCATCAACACCGAGTT-3'
	Reverse	5'- CTTTGTGCGTTGGTTAGCTGGT-3'
snail	Forward	5'- TCGGAAGCCTAACTACAGCGA-3'
	Reverse	5'- AGATGAGCATTGGCAGCGAG-3'
slug	Forward	5'- CGAACTGGACACACATACAGTG-3'
	Reverse	5'- CTGAGGATCTCTGGTTGTGGT-3'
c-myc	Forward	5'- GGCTCCTGGCAAAGGTCA-3'
	Reverse	5'- CTGCGTAGTTGTGCTGATGT-3'
cyclinD1	Forward	5'- GCTGCGAAGTGGAACCATC-3'
	Reverse	5'- CCTCCTTCTGCACACATTTGAA-3'
β-actin	Forward	5'- CATGTACGTTGCTATCCAGGC-3'
	Reverse	5'- CTCCTTAATGTCACGCACGAT-3'